Article citation info:
Lakikza A, Cheghib H, Kahoul N. Diagnosis of bearing faults in wind turbine systems using vibrational signal processing and machine learning. Diagnostyka. 2024;25(3):2024307. https://doi.org/10.29354/diag/191393.

DIAGNOSTYKA, 2024, Vol. 25, No. 3

e-ISSN 2449-5220
DOI: 10.29354/diag/191393

DIAGNOSIS OF BEARING FAULTS IN WIND TURBINE SYSTEMS USING VIBRATIONAL SIGNAL PROCESSING AND MACHINE LEARNING

Abderrahmane LAKIKZA [*], **Hocine CHEGHIB**, **Nabil KAHOUL**

Electromechanical Systems Laboratory, Badji Mokhtar-Annaba University, Algeria
[*] Corresponding author, e-mail: abderrahmane.lakikza@univ-annaba.dz

Abstract

This study employs an integrated methodology for the analysis and diagnosis of bearing faults in rotating machinery and wind turbine systems. The methodology begins by analyzing the original signal using Variational Mode Decomposition to extract distinct modes. Subsequently, the envelope is derived from the optimal mode and transformed into the frequency domain using Fast Fourier Transform to compute the envelope spectrum. The spectrum is segmented into specific frequency bands, and the energy within each band is quantified as features for training a K Nearest Neighbors classification model. The dataset is partitioned into training and testing subsets using cross-validation, and model performance is assessed using metrics such as accuracy and F1 score to ensure robust diagnostic capabilities. Comparative analysis of frequency spectra from real wind turbine signals highlights improvements in energy localization and distribution post-envelope processing. The proposed methodology is then applied to classify faults using the Case Western Reserve University dataset, demonstrating significant enhancements in diagnostic accuracy. These findings underscore the efficacy of the methodology in advancing fault diagnosis in complex machinery systems.

Keywords: wind turbine bearing fault, diagnosis, vibrational signal processing, K-Nearest Neighbors

List of Symbols/Acronyms

CEEMDAN – Complete Ensemble Empirical Mode Decomposition with Adaptive Noise;
d – The diameter of rolling element;
D – The pitch diameter;
DWT – Discrete Wavelet Transform;
EEMD – Ensemble Empirical Mode Decomposition;
FFT – Fast Fourier Transform;
i – The imaginary unit;
IMF – Intrinsic Mode Function;
N – sample size;
VMD – Variational Mode Decomposition;
x(n) – samples;
X(t) – The original signal;
β – contact angle.
E – The expectation operator;
Fi – Fault Frequency of inner race;
$\delta(t)$ – The Dirac functions;
$\|\|_2^2$ – The L2 norm;
* – The convolution operation;
F_0 – Rotation Frequency;
$u_k(t)$ – The intrinsic mode function (IMF);
$\bar{x}$ – the mean;
ω_k – entered frequency.

1. INTRODUCTION

In the contemporary era, where energy demands continue to rise, wind power has emerged as a substantial contributor to the renewable energy sector. The global installed capacity reached approximately 599 gigawatts in 2018, constituting a significant 25% of the world's electrical energy production from renewable sources [22][32]. Conversely, the operation and maintenance of wind turbines account for a substantial 35% of the overall costs [10]. The efficiency of this energy production is intricately linked to the condition of the system, necessitating a focus on enhancing operating conditions and implementing preventive maintenance measures to mitigate potential failures. Within the domain of wind turbines, researchers grapple with a spectrum of challenges posed by various types of faults, encompassing gearbox faults [12], generator faults [19], blade irregularities, and rotor malfunctions [20]. Among these, bearing failures have garnered particular attention due to their critical role as pivotal components within the wind turbine system [3][20].

On the diagnostic front, a myriad of methods is employed to monitor and address these faults. This comprehensive approach includes the analysis of

Received 2023-12-18; Accepted 2024-07-18; Available online 2024-08-20

vibration signals [8] and current signals [28], utilizing a diverse array of mathematical tools and classifier methods such as Artificial Neural Networks [9], K-Nearest Neighbors [15][21], and various machine learning and deep learning techniques [1][26].

Numerous investigations have illuminated the efficiency of diagnosing and monitoring wind turbine systems through a meticulous analysis of vibration signals [33][8], spanning both their time and frequency domains. These signals encapsulate a wealth of information crucial for assessing the system's state.

In the time domain, foundational metrics such as kurtosis, skewness, crest factor [2], and RMS [10] serve as pivotal indicators for monitoring system health. The transition from the time domain to the frequency domain is paramount for a nuanced analysis and diagnostics. Essential tools like the Fast Fourier Transform (FFT) [24] play a crucial role in this transition, enabling a more accurate examination of the signal's frequency components. A notable addition to this diagnostic framework is Spectral Kurtosis (SK), a measure of the non-Gaussianity of frequency components within the signal. Remarkably, SK emerges as a valuable technique specifically adept at monitoring wind turbine bearing failure [8]. As the analysis process advances towards heightened precision, it relies on an array of sophisticated filtering tools, including band-pass, low-pass, high-pass, and noise reduction methodologies. Among these tools, the pivotal Discrete Wavelet Transform (DWT) [4] stands out, recognized for its efficacy in enhancing signal clarity. Complementing these filtering techniques are mathematical tools adept at processing non-linear and non-stationary signals, introducing a layer of complexity to the diagnostic approach. Noteworthy among these mathematical tools are Variational Mode Decomposition (VMD) [33], Empirical Mode Decomposition (EMD) [17], Complete Ensemble Empirical Mode Decomposition with Adaptive Noise (CEEMDAN) [8], and various others [26].

These integral components contribute not only to the precision of the diagnostic process but also to a deeper understanding of the nuanced dynamics inherent in wind turbine systems. As we navigate through the intricacies of signal processing, the judicious use of these filtering and mathematical tools emerges as a cornerstone in unraveling the complexities associated with wind turbine health and performance.

Signal processing, paired with a machine learning model emulating the intricacies of human cognition, stands as a transformative force in fault diagnosis. This research [15] leveraged the Wavelet Transform (WT) and Hilbert Huang Transform (HHT) in conjunction with the K-Nearest Neighbors (KNN) algorithm for wind turbine fault diagnosis. The evaluation incorporated performance metrics, such as Root Mean Square Error (RMSE) and Mean Square Error (MSE), to assess the effectiveness of their proposed approach. The obtained results demonstrated the efficacy of the methodology, yielding satisfactory outcomes in the study. This paper [21] seamlessly combined VMD and singular value decomposition (SVD) techniques for extracting frequency features, while integrating the K-Nearest Neighbors (KNN) algorithm to enhance fault classification in rotation machinery. This unified approach showcased improved accuracy and reliability in fault diagnosis.

In this paper, VMD analysis was used to extract an optimal signal that represents fault characteristics. Subsequently, a feature extraction method from the envelope spectrum of the signal was integrated, focusing on the frequency energy for each band from 0 to 500 Hz, where bearing fault frequencies are typically located. This range was divided into five bands, with each band's frequency energy value representing a feature. These features were then used with a KNN model for fault diagnosis, aiming to enhance classification accuracy by improving the feature source prior to algorithm optimization.

2. METHODS AND MATERIALS

2.1. Variational Mode Decomposition

The VMD method is used in this work to process non-linear, non-stationary signals for diagnosing faults in rotating machines, in particular bearing faults in wind turbines [33]. It decomposes the signal into sub-signals called "IMF" based on known initial conditions (α (penalty factor), τ (relative tolerance), k (number of IMFs), max iteration) as are represented by the following equations.

$$\mathrm{X(t)} = \sum_{k=1}^{K} u_k(t) \tag{1}$$

To obtain the unilateral spectrum of the IMF, we use the Hilbert transform as described below [31][32]:

$$\left[\delta(t) + \frac{i}{\pi t}\right] * u_k(t) e^{-i\omega_k t} \tag{2}$$

The fundamental question of the VMD algorithm is how to obtain the solution of the variational problem, which is formulated in equation (5) as follows [27]:

$$\min_{\{u_k\},\{\omega_k\}} \left\{ \sum_k ||\partial_t[\left(\delta(t) + \frac{i}{\pi t}\right) * u_k(t)] e^{-i\omega_k t}||_2^2 \right\} \tag{3}$$

To solve the variational model, we introduce the Lagrange multiplier λ(t) and the penalty factors α [30 - 31], The augmented Lagrange function is expressed as follows:

$$L(\{u_k\},\{\omega_k\},\{\lambda(t)\}) = \alpha \sum_{k=1}^{K} ||\partial_t[\left(\delta(t) + \frac{i}{\pi t}\right) * u_k(t)] e^{-i\omega_k t}||_2^2 + ||f(t) - \sum_{k=1}^{K} u_k(t)||_2^2 + \langle \lambda(t), f(t) - \sum_{k=1}^{K} u_k(t) \rangle \tag{4}$$

We then update factors u_k, ω_k and $\lambda(t)$ iteratively until we reach the optimal solution, The algorithm aims to satisfy the convergence condition [22].

2.2. Data base

a. Wind turbine bearing database

The dataset [25] was collected from a 2 MW wind turbine high-speed shaft driven by a 20-tooth pinion gear [5]. A vibration signal was acquired for 6 seconds daily over a period of 50 consecutive days. An inner race fault developed and caused bearing failure throughout the 50-day period. The sampling rate was 97657 samples per second for 6 seconds.

The data depicts the variation in speed of a high-speed shaft on a wind turbine over a 6-second interval. The shaft's speed fluctuates between its minimum and maximum values, showcasing a change of 3.6%. This variability can impact the spectral characteristics of bearing fault frequencies, including cage, ball, inner race, and outer race rates, as detailed in the following table.

Table 1. Wind turbine bearing rates

Shaft\Bearing Fault frequency	Cage	Ball	Inner race	Outer race
Low: 30.9 (Hz)	12.98	88.69	292.3	207.7
High: 32.01 (Hz)	13.44	91.88	302.8	215.1

The data used in the application of the signal analysis methodology consists of two signals: the healthy condition signal and the signals from April 20 to April 25 (as the fault develops and the characteristics of the fault become more detailed in the later days). (The database used is MATLAB Data (.mat)).

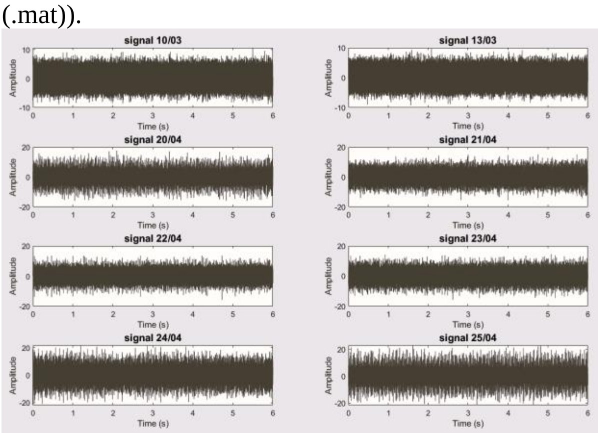

Fig. 1. The signals used

b. Case Western Reserve university database

The CWRU database [7] is a renowned collection of mechanical vibration datasets used for evaluating bearing system performance and diagnosing faults. It includes multiple datasets with detailed information on fault conditions and healthy states. Table 2 outlines various fault characteristics recorded, while Table 3 details how the test data was prepared for our study.

2.3. The proposed methods

Variational Mode Decomposition is included to ensure optimized data for advanced analysis.

Table 2. CWRU bearing information

Drive end bearing 6205-2RS JEM SKF (Fault Types)	Cage	Ball	Inner race	Outer race
Fault frequencies (Hz)	11.9 (Hz)	141.2 (Hz)	162.2 (Hz)	107.4 (Hz)

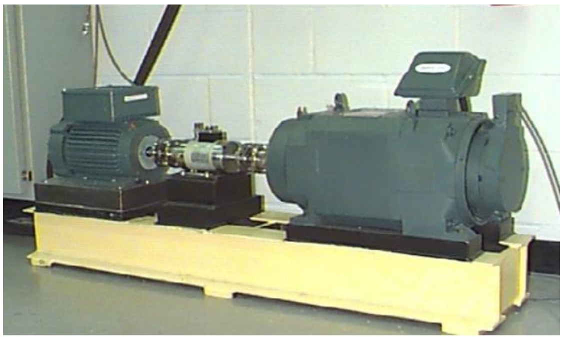

Fig. 2. The test bench

Table 3. CWRU database description

Fault type	Inner race fault	Ball fault	Outer race fault	Healthy condition
Operating speed (rpm)	1797 1772	1797 1772	1797	1797
Diameter (inch)	0.007’	0.007’	0.007’	0.007’
Number of signals	2	2	3	1
Number of sub signals	30	30	45	30
Samples per sub signals	8000	8000	8000	8000

To extract the optimal IMF, many techniques are used to study and evaluate the quality of the modes obtained, such as Kurtosis, correlation, entropy values factor [2][6] [30 - 31].

We propose the mean kurtosis and RMSE to select the optimal mode.

Note that the mathematical expression for kurtosis and RMSE is as follows in order [16]:

$$Ku = \frac{1}{N}\frac{\sum_{n=1}^{N}(x(n)-\bar{x})^4}{[(\frac{1}{N})\sum_{n=1}^{N}(x(n)-\bar{x})^2]^2} \quad (5)$$

$$RMSE = \sqrt{(\frac{1}{N}\sum_{i=1}^{N}(S_i - S'_i)^2)} \quad (6)$$

Where the S_i and S'_i represent the values of the signals.

Then, we apply an Envelope Hilbert transform to enable spectral analysis and observe the manifestation of vibrational energy related to the defect. The Hilbert transform equation is given in the following two formulations [13][14]:

$$H[x(t)] = x(t) * \frac{1}{\pi t} \quad (7)$$

$$H[x(t)] = \frac{1}{\pi}\int_{-\infty}^{\infty}\frac{X(\tau)}{t-\tau}\,d\tau \quad (8)$$

The bearing failure frequencies formulae are given as below [6], where N is the angular velocity of the rotor:

$$Fi = \frac{n}{2}\frac{N}{60}\left(1 + \frac{d}{D}\cos\beta\right) \quad (9)$$

$$Fo = \frac{n}{2}\frac{N}{60}\left(1 - \frac{d}{D}\cos\beta\right) \quad (10)$$

$$Fre = \frac{n}{2d}\frac{N}{60}\left(1 - (\frac{d}{D}\cos\beta)^2\right) \quad (11)$$

$$Fc = \frac{N}{2\times 60}\left(1 - \frac{d}{D}\cos\beta\right) \quad (12)$$

The proposed approach is shown in the Fig. 3.

Description of proposed approach:

- Step 1: The VMD method is used to decompose the signals according to appropriate criteria [α (2000), τ (0.005), k (5), max iteration=500].
- Step 2: We extract the optimal IMF using the mean kurtosis of IMFs and RMSE.
- Step 3: Obtain the Envelope and analyze the results.

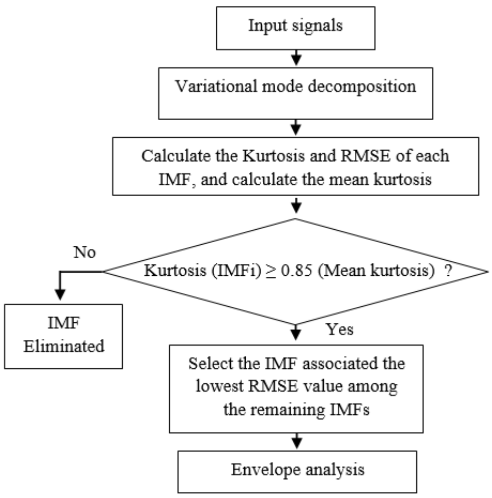

Fig. 3. The proposed approach

Additionally, we employ machine learning for diagnosis through KNN following the approach illustrated in the Fig.4.

The KNN classification algorithm relies on finding the nearest neighbors for the test sample. When a test sample is provided, the algorithm searches the pattern space to locate the K training samples closest to it, and then calculates the distances to these neighbors. If a particular class has the maximum number of nearest neighbors, the test sample is classified into that class.[15][21]

Methodology for Fault Diagnosis Using Nearest Neighbors:

- Step 1: Collect the vibrational signals during different operational states, including normal operation, inner race faults, ball fault and outer race fault scenarios, after processing them following the proposed approach using VMD we obtain the envelope for each signal.
- Step 2: Calculate Frequency Domain Energy using the following steps:

1. Use the FFT function in MATLAB to transform the signal.
2. Compute the absolute value of the frequency spectrum.
3. Define the frequency bands (Hz) [0, 100], [100, 200], [200, 300], [300, 400], [400, 500].
4. Use the FFT of the signal to calculate the energy in these bands by summing the squared frequency values.

Represent the data in a matrix X where rows correspond to signals and columns to extracted features.

- Step 3: Use MATLAB's (fitcknn) to train the KNN model on the labelled insurance dataset, which includes: Healthy, inner race fault, ball fault and outer race fault.
- Step 4: Evaluate the trained KNN model using a separate set of labeled test data to assess its generalization performance.

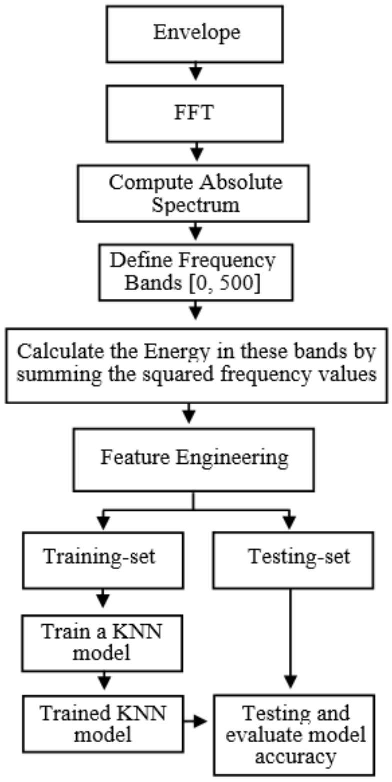

Fig. 4. The proposed method for KNN classification

3. RESULTS AND DISCUSION

We apply the methodology illustrated in Figure 3 to wind turbine bearing signals to compare the results with the envelope of the original signals.

Fig 5 illustrates the envelope spectrums of the original signals.

Next, we apply VMD to the eight signals and extract the optimal mode based on RMSE values and kurtosis. The results are presented in the following table 4.

When comparing the envelope spectrum before and after processing using Variational Mode Decomposition, we notice some significant changes in the energy representation of the signal. Before processing, the original envelope spectrum contains a variety of peaks that may represent true signals, noise, or unwanted interferences, and the energy is distributed across a wide range of frequencies,

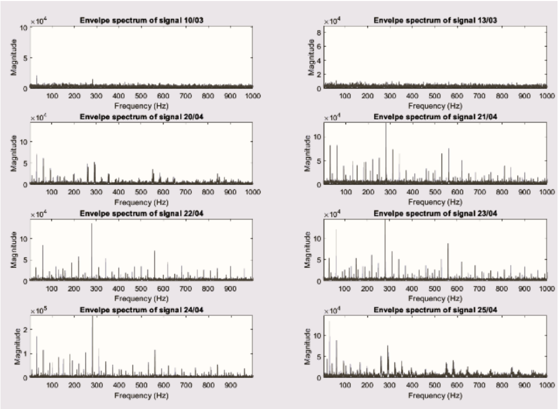

Fig. 5. Envelope spectrum of the signals before processing

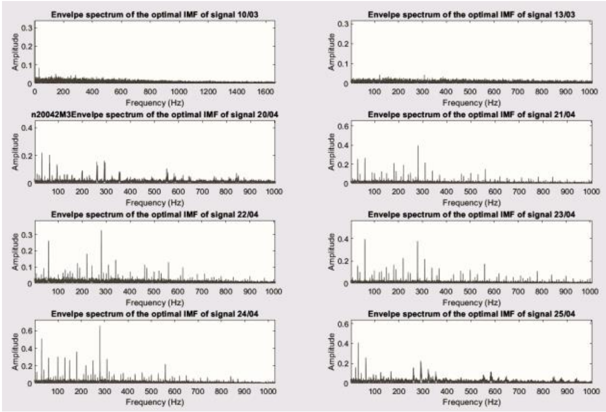

Fig. 6. Envelope spectrum of the IMFs selected

Table 4. Kurtosis and RMSE values for each IMF

Signals	IMFs	Kurtosis	RMSE
Signal 10/03	1	3.059	1.921
	2	3.074	1.437
	3	2.988	1.606
	4	2.979	1.866
	5	2.946	1.955
Signal 13/03	1	3.007	1.886
	2	3.015	1.497
	3	3.020	1.488
	4	2.960	1.828
	5	2.966	1.918
Signal 20/04	1	3.454	2.246
	2	4.466	2.066
	3	5.768	1.603
	4	3.014	2.234
	5	2.970	2.244
Signal 21/04	1	3.541	2.387
	2	4.449	1.807
	3	4.435	1.868
	4	3.146	2.330
	5	2.976	2.355
Signal 22/04	1	3.374	2.185
	2	5.699	2.087
	3	3.875	1.688
	4	3.859	1.821
	5	3.000	2.141
Signal 23/04	1	3.496	2.348
	2	4.492	1.771
	3	4.073	1.808
	4	3.043	2.321
	5	2.983	2.399
Signal 24/04	1	3.211	3.116
	2	5.250	2.197
	3	5.374	2.343
	4	3.251	3.034
	5	2.976	3.058
Signal 25/04	1	3.218	2.885
	2	4.103	2.647
	3	5.643	2.013
	4	5.799	2.567
	5	2.983	2.807

Fig. 6 represents the envelope spectrum signal of each IMF selected.

making it difficult to identify important features. After applying VMD, the energy is redistributed to concentrate in specific frequency bands that correspond to the extracted modes. The peaks that were previously obscured by noise or interferences become more prominent and clearer, making it easier to identify important frequency features. The goal is to improve the signal for feature extraction in the frequency range of 0 to 500 Hz.

Table 5. Frequency energy values for each processed envelope signal in specified frequency bands: Signals (10/03; 13/03; 20/04; 21/04; 22/04; 23/04; 24/04; 25/04)

[0,100] Hz	[100,200] Hz	[200,300] Hz	[300,400] Hz	[400,500] Hz
2.30	0.155	0.140	0.123	0.095
1.727	0.095	0.082	0.078	0.070
3.543	0.258	0.428	0.224	0.148
3.088	0.272	0.455	0.211	0.152
2.568	0.214	0.305	0.186	0.153
3.046	0.264	0.438	0.217	0.143
5.703	0.634	1.351	0.470	0.326
5.464	0.523	1.045	0.624	0.237

Table 6. Frequency energy values for original envelope signals in specified frequency bands: Signals (10/03; 13/03; 20/04; 21/04; 22/04; 23/04; 24/04 ;25/04)

[0,100] Hz	[100,200] Hz	[200,300] Hz	[300,400] Hz	[400,500] Hz
6.454	0.110	0.111	0.094	0.083
6.236	0.093	0.085	0.078	0.082
8.748	0.235	0.447	0.206	0.121
9.458	0.272	0.735	0.289	0.198
8.073	0.198	0.401	0.188	0.166
9.296	0.2620	0.616	0.285	0.188
15.01	0.641	2.331	0.738	0.434
13.26	0.479	1.254	0.597	0.257

Through the tables (5.6), we observe clear distinctions between the values of faulty and healthy signals. Additionally, we notice that the proximity of values for the inner race fault in the processed signal indicates improved accuracy in diagnosis and classification.

Based on the prepared data of Case Western Reserve University as mentioned in section (2.2), we divide the data into 80% for training and 20% for testing. We repeat this process five times, alternating between training and testing datasets. Prior to using the proposed methodology, the results were inaccurate (27% accuracy). After implementing the methodology, the results significantly improved, as detailed below.

The faults in these data were diagnosed using the Improved Grey Wolf Optimizer SVM method [23], achieving a high accuracy of 98.71%, whereas the proposed methodology yielded a classification accuracy of 98.81% in handling this data.

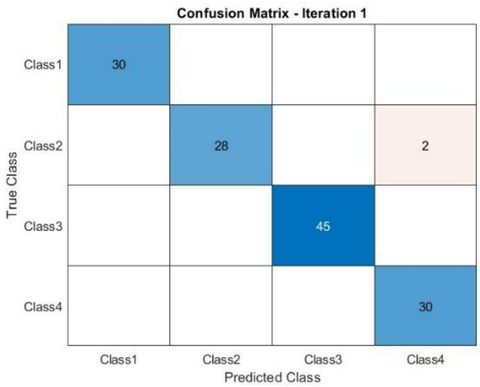

Fig. 7. Confusion matrix-iteration 1

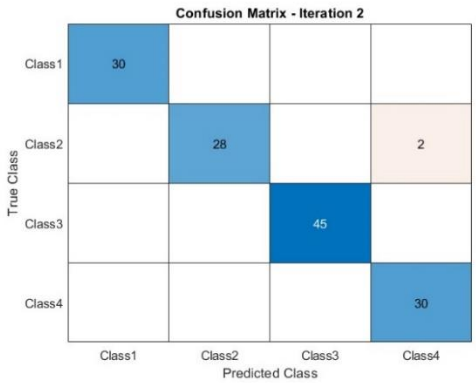

Fig. 8. Confusion matrix-iteration 2

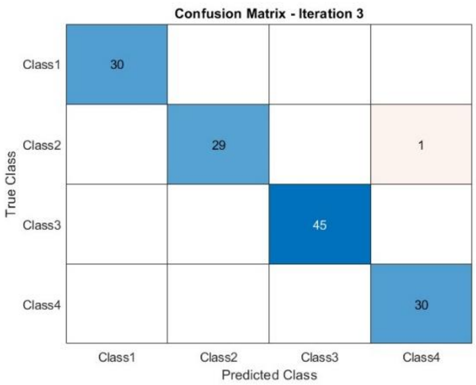

Fig. 9. Confusion matrix-iteration 3

5. CONCLUSION

This research was conducted in sequential stages to analyze and diagnose bearing faults in wind turbine systems using Variational Mode Decomposition and KNN classification. After applying VMD to the signals, filtered signals representing optimal modes for each signal were obtained. These modes were utilized to extract the envelope and compute the envelope spectrum for the eight conditions of wind turbine signals.

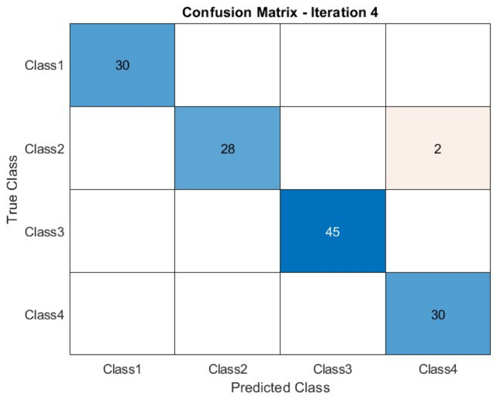

Fig. 10. Confusion matrix-iteration 4

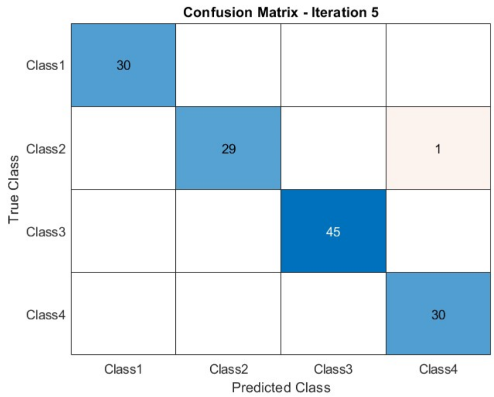

Fig. 11. Confusion matrix-iteration 5

We observed improvements in energy concentration and distribution among different fault conditions. Frequency energy was extracted by dividing the envelope spectrum into ranges from 0 to 100 Hz, 100 to 200 Hz, 200 to 300 Hz, 300 to 400 Hz and 400 to 500Hz. We observed convergence in energy values for the fault condition within these ranges, indicating high accuracy in classification.

The developed model of KNN was tested using the CWRU dataset, where the model demonstrated good performance with an accuracy of 98.81% and an F1 score of 98.72%. These results confirm the model's capability to effectively handle fault classifications and accurately identify fault conditions.

Future work could propose further enhancement of the method through algorithmic refinement of VMD partitioning and extraction of more precise features, applying them to more complex scenarios.

Source of funding: *This research received no external funding.*

Author contributions: *research concept and design, A.L., H.C., N.K.; Collection and/or assembly of data, A.L.,* *H.C., N.K.; Data analysis and interpretation, A.L., H.C., N.K.; Writing the article, A.L., H.C., N.K.; Critical revision of the article, A.L., H.C., N.K.; Final approval of the article, A.L., H.C., N.K.*

Declaration of competing interest: *The authors declare that they have no known competing financial interests or personal relationships that could have appeared to influence the work reported in this paper.*

REFERENCES

1. Adlen K, Ridha K. Recurrent neural network optimization for wind turbine condition prognosis. Diagnostyka 2022; 23(3): 1–11. https://doi.org/10.29354/diag/151608.
2. An G, Tong Q, Zhang Y, Liu R, Li W, Cao J, et al. An improved variational mode decomposition and its application on fault feature extraction of rolling element bearing. Energies 2021; 14(4): 1079. https://doi.org/10.3390/en14041079.
3. Lu B, Li Y, Wu X, Yang Z. A review of recent advances in wind turbine condition monitoring and fault diagnosis. 2009 IEEE Power Electronics and Machines in Wind Applications 2009; 1–7. https://doi.org/10.1109/PEMWA.2009.5208325.
4. Bakir T, Boussaid B, Hamdaoui R, Abdelkrim MN, Aubrun C. Fault detection in wind turbine system using wavelet transform: Multi-resolution analysis. 2015 IEEE 12th International Multi-Conference on Systems, Signals & Devices (SSD15) 2015; 1–6. https://doi.org/10.1109/SSD.2015.7348223.
5. Bechhoefer E, Van Hecke B, He D. Processing for improved spectral analysis. Annual Conference of the PHM Society 2013; 5(1) https://doi.org/10.36001/phmconf.2013.v5i1.2220.
6. Bouaouiche K, Menasria Y, Khalfa D. Detection of defects in a bearing by analysis of vibration signals. Diagnostyka 2023; 24(2): 1–7. https://doi.org/10.29354/diag/162230.
7. CWRU. Vibration Database. Case Western Reserve University, 2023. https://engineering.case.edu/bearingdatacenter/download-data-file.
8. Djemili I, Medoued A, Soufi Y. A wind turbine bearing fault detection method based on improved CEEMDAN and AR-MEDA. Journal of Vibration Engineering & Technologies 2024; 12(3): 4225–46. https://doi.org/10.1007/s42417-023-01117-x.
9. Encalada-Dávila Á, Puruncajas B, Tutivén C, Vidal Y. Wind turbine main bearing fault prognosis based solely on SCADA Data. Sensors 2021; 21(6): 2228. https://doi.org/10.3390/s21062228.
10. Gao Z, Liu X. An Overview on fault diagnosis, prognosis and resilient control for wind turbine systems. Processes 2021;9(2):300. https://doi.org/10.3390/pr9020300.
11. Leite GDNP, Araújo AM, Rosas PAC, Stosic T, Stosic B. Entropy measures for early detection of bearing faults. Physica A: Statistical Mechanics and its Applications 2019; 514: 458–72. https://doi.org/10.1016/j.physa.2018.09.052.
12. Gu H, Liu WY, Gao QW, Zhang Y. A review on wind turbines gearbox fault diagnosis methods. Journal of Vibroengineering 2021; 23(1): 26–43. https://doi.org/10.21595/jve.2020.20178.
13. Wang J, Qiao L, Ye Y, Chen Y. Fractional envelope analysis for rolling element bearing weak fault feature extraction. IEEE/CAA Journal of Automatica Sinica 2017; 4(2): 353–60. https://doi.org/10.1109/JAS.2016.7510166.
14. Bouaouiche K, Menasria Y, Khalfa D. Detection and diagnosis of bearing defects using vibration signal processing. Archive of Mechanical Engineering 2023: 433–52. https://doi.org/10.24425/ame.2023.146849.
15. Malik H. Wavelet and Hilbert Huang transform based wind turbine imbalance fault classification model using k-nearest neighbour algorithm. International Journal of Renewable Energy Technology 2018; 9(1/2):66. https://doi.org/10.1504/IJRET.2018.090105.
16. Xiao M, Wen K, Zhang C, Zhao X, Wei W, Wu D. Research on fault feature extraction method of rolling bearing based on NMD and wavelet threshold denoising. Shock and Vibration. 2018(1): 9495265. https://doi.org/10.1155/2018/9495265.
17. Meng D, Wang H, Yang S, Lv Z, Hu Z, Wang Z. Fault analysis of wind power rolling bearing based on EMD feature extraction. Computer Modeling in Engineering & Sciences 2022;130(1):543–58. https://doi.org/10.32604/cmes.2022.018123.
18. Niesłony A, Böhm M, Owsiński R. Crest factor and kurtosis parameter under vibrational random loading. International Journal of Fatigue 2021; 147: 106179. https://doi.org/10.1016/j.ijfatigue.2021.106179.
19. Olabi AG, Wilberforce T, Elsaid K, Sayed ET, Salameh T, Abdelkareem MA, et al. A Review on failure modes of wind turbine components. Energies 2021; 14(17): 5241. https://doi.org/10.3390/en14175241.
20. Peng H, Zhang H, Fan Y, Shangguan L, Yang Y. A review of research on wind turbine bearings' failure analysis and fault diagnosis. Lubricants 2022; 11(1):14. https://doi.org/10.3390/lubricants11010014.
21. Lu Q, Shen X, Wang X, Li M, Li J, Zhang M. Fault diagnosis of rolling bearing based on improved VMD and KNN. Mathematical Problems in Engineering. 2021; 2021: 1–11. https://doi.org/10.1155/2021/2530315.
22. Ahmed SD, Al-Ismail FSM, Shafiullah M, Al-Sulaiman FA, El-Amin IM. Grid integration challenges of wind energy: A Review. IEEE Access 2020; 8: 10857–78. https://doi.org/10.1109/ACCESS.2020.2964896.
23. Shen W, Xiao M, Wang Z, Song X. Rolling bearing fault diagnosis based on support vector machine optimized by improved grey Wolf algorithm. Sensors 2023; 23(14): 6645. https://doi.org/10.3390/s23146645.
24. Strömbergsson D, Marklund P, Berglund K, Larsson P. Bearing monitoring in the wind turbine drivetrain: A comparative study of the FFT and wavelet transforms. Wind Energy 2020; 23(6): 1381–93. https://doi.org/10.1002/we.2491.
25. The data is available on this website: https://github.com/mathworks/WindTurbineHighSpeedBearingPrognosis-Data
26. Liu WY, Tang BP, Han JG, Lu XN, Hu NN, He ZZ. The structure healthy condition monitoring and fault diagnosis methods in wind turbines: A review. Renewable and Sustainable Energy Reviews 2015; 44: 466–72. https://doi.org/10.1016/j.rser.2014.12.005.
27. Wang X, Ruan J, Zhou T, Peng X, Deng Y, Yang Q. Data mining in the vibration signal of the trip mechanism in circuit breakers based on VMD-PSR.

Electronics 2022; 11(22): 3700. https://doi.org/10.3390/electronics11223700.
28. Gong X, Qiao W. Bearing fault detection for direct-drive wind turbines via stator current spectrum analysis. 2011 IEEE Energy Conversion Congress and Exposition, Phoenix, AZ, USA, 2011; 313-318. https://doi.org/10.1049/iet-rpg.2012.0278.
29. Zhang Y, Zhang C, Liu , Wang W, Han Y, Wu N. Fault diagnosis method of wind turbine bearing based on improved intrinsic time-scale decomposition and spectral Kurtosis. 2019 Eleventh International Conference on Advanced Computational Intelligence (ICACI), Guilin, China, 2019;29-34. https://doi.org/10.1109/TEC.2012.2227746.
30. Yang J, Zhou C, Li X. Research on fault feature extraction method based on parameter optimized variational mode decomposition and robust independent component analysis. Coatings 2022; 12(3): 419. https://doi.org/10.3390/coatings12030419.
31. Yang J, Zhou C, Li X, Pan A, Yang T. A fault feature extraction method based on improved VMD multi-scale dispersion entropy and TVD-CYCBD. Entropy 2023;25(2):277. https://doi.org/10.3390/e25020277.
32. Zhang F, Chen M, Zhu Y, Zhang K, Li Q. A Review of fault diagnosis, status prediction, and evaluation technology for wind turbines. Energies 2023; 16(3): 1125. https://doi.org/10.3390/en16031125.
33. Zhao H, Li L. Fault diagnosis of wind turbine bearing based on variational mode decomposition and Teager energy operator. IET Renewable Power Generation 2017; 11(4): 453–60. https://doi.org/10.1049/iet-rpg.2016.0070.

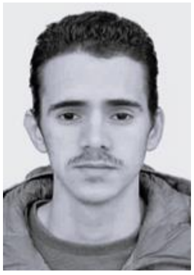

Abderrahmane LAKIKZA
Holder of a bachelor's and master's degree in industrial maintenance from the University of Skikda in 2021. Currently, a Ph.D. student at the University of Badji Mokhtar Annaba in Algeria, specializing in Industrial Maintenance, and affiliated with the Electromechanical Systems Laboratory (LSELM), Annaba. Particularly interested in diagnosing failures in wind turbine systems.
e-mail : abderrahmane.lakikza@univ-annaba.dz

Hocine CHEGHIB
e-mail: cheghib_h@yahoo.fr

Nabil KAHOUL
e-mial: nabil_ka@yahoo.fr